

## Article

# A Co-Simulation Model Integrating a Musculoskeletal Human Model with Exoskeleton and Power Tool Model

Carla Molz <sup>1</sup>, David Scherb <sup>1</sup>, Christopher Löffelmann <sup>1</sup>, Johannes Sänger <sup>2</sup>, Zhejun Yao <sup>3</sup>,  
Andreas Lindenmann <sup>2</sup>, Sven Matthiesen <sup>2</sup>, Robert Weidner <sup>3,4</sup>, Sandro Wartzack <sup>1</sup> and Jörg Miehling <sup>1,\*</sup>

<sup>1</sup> Engineering Design, Friedrich-Alexander-Universität Erlangen-Nürnberg (FAU), Martensstraße 9, 91058 Erlangen, Germany; molz@mfk.fau.de (C.M.); scherb@mfk.fau.de (D.S.); christopher.loeffelmann@fau.de (C.L.); wartzack@mfk.fau.de (S.W.)

<sup>2</sup> Karlsruhe Institute of Technology (KIT), IPEK—Institute of Product Engineering, Kaiserstraße 10, 76131 Karlsruhe, Germany; johannes.saenger@kit.edu (J.S.); andreas.lindenmann@kit.edu (A.L.); sven.matthiesen@kit.edu (S.M.)

<sup>3</sup> Laboratory of Manufacturing Technology, Helmut Schmidt University (HSU), Holstenhofweg 85, 22043 Hamburg, Germany; zhejun.yao@hsu-hh.de (Z.Y.); robert.weidner@hsu-hh.de (R.W.)

<sup>4</sup> Chair for Production Technology, Institute of Mechatronics, University of Innsbruck (UIBK), Technikerstraße 13, 6020 Innsbruck, Austria

\* Correspondence: miehling@mfk.fau.de

**Featured Application:** This research aims to provide a co-simulation model to derive design optimizations for technical support systems regarding the user needs.

**Abstract:** Working at and above head height with a power tool represents a common activity in craft and assembly applications. To assist and protect the user from overload and injuries in these situations, the development and use of application-specific support systems, such as exoskeletons and power tools, have greatly increased in recent years. Thus, the integration of aspects of the user-centered product development of support systems in the early phases of product development process has high potentials. A common approach to integrate the user early in the product development process is the use of musculoskeletal human models, which allow the evaluation of effects on the human body. This could also be applicable in the mentioned use case to enable the evaluation of the interactions for the user. Therefore, a co-simulation model for virtual modelling and simulating human–machine interactions is presented. The co-simulation model is made up of a musculoskeletal human model and the models of the technical systems (exoskeleton and power tool). By applying the co-simulation model, the impact of technical systems on the human body can be taken into account to derive design alternatives for the technical system due to the requirements of the user. The paper describes the design of the co-simulation model and particularly, the interaction of the submodels. The evaluation of the co-simulation model is carried out with the help of a subject study for the selected use case working at and above head height. The results show plausible results for the muscle loads considering the support by an exoskeleton. Furthermore, the comparison of simulated results to measured muscle activations via surface electromyography shows a good agreement. Thus, the co-simulation model passes the test for functionality and seems to be applicable for the derivation of design alternatives of technical systems regarding the user needs. In future, the co-simulation model will be further validated with a higher number of subjects and to implement design alterations in the technical systems.

**Keywords:** human–machine interaction; biomechanics; support systems; exoskeleton; product development; user-centered design; musculoskeletal human model



**Citation:** Molz, C.; Scherb, D.; Löffelmann, C.; Sänger, J.; Yao, Z.; Lindenmann, A.; Matthiesen, S.; Weidner, R.; Wartzack, S.; Miehling, J. A Co-Simulation Model Integrating a Musculoskeletal Human Model with Exoskeleton and Power Tool Model. *Appl. Sci.* **2024**, *14*, 2573. <https://doi.org/10.3390/app14062573>

Academic Editor: Heecheon You

Received: 1 February 2024

Revised: 12 March 2024

Accepted: 15 March 2024

Published: 19 March 2024



**Copyright:** © 2024 by the authors. Licensee MDPI, Basel, Switzerland. This article is an open access article distributed under the terms and conditions of the Creative Commons Attribution (CC BY) license (<https://creativecommons.org/licenses/by/4.0/>).

## 1. Introduction

Due to the increasing attention to health and well-being in the workplace, the interest in support systems, such as exoskeletons and power tools, for workers in these situations is

growing. Such systems can be used in physically demanding work situations and thus reduce the user's physical stress at the workplace [1–4]. For the development of such systems, the interaction with the user is of great importance, as these systems are in direct force and information transmission with the human [5,6]. However, studies with subjects and prototypes or test benches [7–10] are still the most commonly used methods for analyzing the effects of the user–product interactions in detail. Due to the extensive interactions of support systems with humans, special attention should be paid to these and the support systems should be developed in a more proactive user-centered way. Wartzack et al. [11] present an approach for the consideration of physiological and psychological aspects of the user–product interaction. In this way, digital human models can be used for virtual evaluation and validation in addition to approaches that map the subjective factors in product development. Depending on the use case, different kinds of digital human models can be used in the product development process. Anthropometric digital human models can map user groups and are typically used in ergonomics assessment for reachability and visibility analyses [12,13]. Due to the representation of the human as a multibody system, musculoskeletal human models are suited for biomechanical analyses. In these models, structures such as bones, tendons and muscles are modelled with particular anatomical accuracy. By using this kind of digital human model, the influence of movements and forces on the human body can be analyzed by using biomechanical parameters such as the muscle activation or joint reaction forces.

In addition to the use of these models for medical applications such as gait analysis [14,15], they are also increasingly being used in product development [16,17]. For example, Rasmussen et al. [18] use musculoskeletal human models for parametric simulations to evaluate different product designs of a saw handle. Furthermore, Peruzzini et al. [19] present an approach for using digital human models in combination with virtual reality in order to support the design of ergonomic workstations.

Moreover, there are already initial approaches for using musculoskeletal human models for the user-centered product development of support systems [20–22]. However, simplifications are often made in these approaches. For example, the exoskeleton's support is simplified as a constant moment acting on a joint [23,24] or as a pure force acting on the bone [25,26]. Thus, principal evaluations due to design concepts or ideas of the support systems can be conducted. Molz et al. [27] show that the influences of user interactions with an exoskeleton and power tool can be mapped by this and possible effects of design changes on the user can be depicted.

Nevertheless, for a more holistic view and a better assessment of design impacts, co-simulation models should be used. On the one hand, this allows for a detailed representation of the user and the products in individual models, whereby simplifications of the individual virtual models can be avoided. On the other hand, interactions between the human and the technical systems can be simulated as realistically as possible. As a result, a co-simulation model can help to represent and quantify the human–machine interactions and their effects on the human body by means of suitable parameters. Based on these parameters, design options for the technical systems, such as the modification of object geometries, can be derived and the user-centered product development process can be supported already in the early phases of product development.

Consequently, we present a co-simulation model integrating a musculoskeletal human model for representing the user and digital models of an exoskeleton and a power tool. A short overview of the idea of this co-simulation model was given by Molz et al. [28]. In the present contribution, we adopt and extend this schematic outline. We present an in-depth description of how this co-simulation model is implemented and how the interactions between the submodels (human, exoskeleton, and power tool) are mapped. Afterwards we implement and evaluate the co-simulation model for the use case “working at and above head height with a cordless screwdriver and the shoulder exoskeleton Lucy [1]”. This use case offers high potential for supporting the user due to the high physical stresses to which the user is exposed to during this activity, especially in the shoulder and neck area [29]. For

this purpose, a case study was conducted to compare simulated results with experimentally determined data.

## 2. Materials and Methods

In order to describe the setup of the co-simulation model, first of all the single elements yielding the complete model are explained. Then, the basic concept and the realized interactions between all submodels are described in detail. Lastly, in order to evaluate the simulation results from the co-simulation model, a design study was conducted with three subjects.

### 2.1. Description of the Submodels

#### 2.1.1. Musculoskeletal Human Model

For implementing the human model and conducting the biomechanical analyses, the open source software OpenSim [30] is used. This software enables the user to model, simulate and analyze the neuromusculoskeletal system of the human with the help of musculoskeletal human models. Various partial body models or full-body models can be used for this purpose. Within the framework of the concept of the co-simulation, we use a full-body model presented by Miehling [31]. The model contains 200 muscle compartments, 40 degrees of freedom and is suitable for inverse and forward dynamic simulations. The model and a simulation of the selected use case of working at and above head height is depicted in Figure 1. By using this model, the influence of technical systems on the whole body can be detected and analyzed by assessing biomechanical parameters such as the muscle activation or joint reaction forces [32,33]. This resulting data can then further be used to derive design alternatives or parameter changes of the technical systems influencing the human body [34–36]. Furthermore, the full-body model setup creates the possibility of a future use of the co-simulation model for different applications or technical systems affecting, for example, the lower extremities.

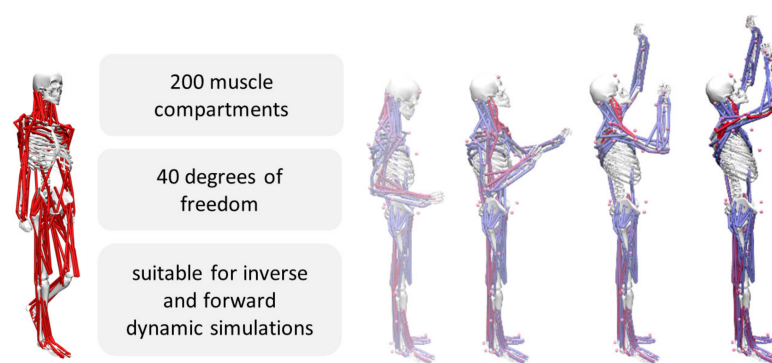


**Figure 1.** Full-body musculoskeletal human model. A full-body model musculoskeletal human model, presented by Miehling et al. [31], is used within the concept of the co-simulation model to conduct biomechanical simulations. On the right side, the load on muscles during an overhead task are shown (red indicates higher loads than blue).

#### 2.1.2. Exoskeleton Model

To simulate the dynamics of human–exoskeleton interaction, an exoskeleton model [37] is built in MATLAB Simscape (R2021b) firstly based on the CAD model of the shoulder exoskeleton Lucy [1]. The exoskeleton Lucy primarily supports the user in working at head level or above (Figure 2). The exoskeleton model replicates the key kinematic and control features of Lucy. It keeps one active joint and two passive joints (white curved arrows in Figure 2) for each exoskeleton arm. Based on the angular movement of the active joint, a control model calculates the force from the cylinder that lifts the exoskeleton’s arm bar. Support level and support profile parameters related to arm motion are included in the control model. To mirror the kinematical adjustments of the exoskeleton, the positions of the

armrests, shoulder bars and lap belt (white straight arrows in Figure 2) are parameterized in the model according to anthropometry.

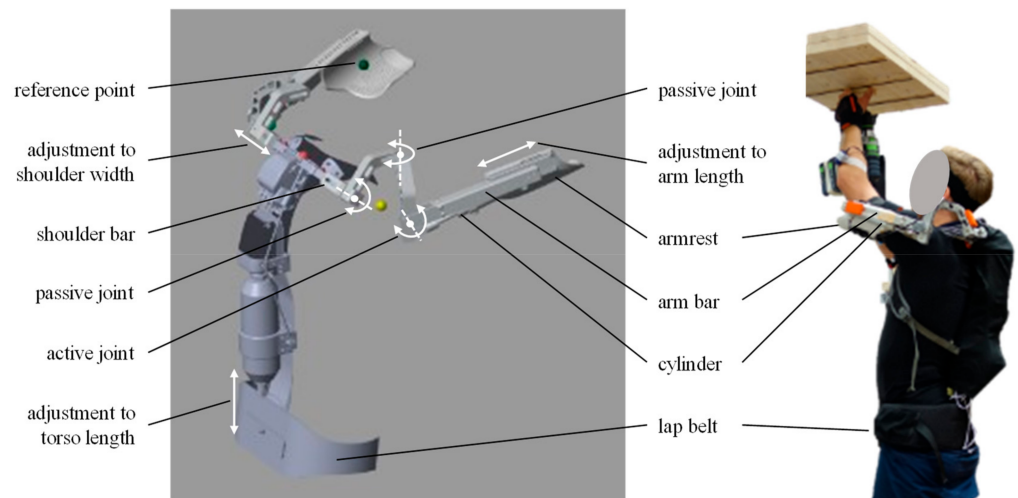


**Figure 2.** Shoulder-exoskeleton Lucy and its multibody model [37]. A multibody model is created for the integration of the exoskeleton into the co-simulation model. The multibody model (left) of the already existing shoulder-exoskeleton Lucy is used for the implementation.

### 2.1.3. Power Tool Model

To simulate the interaction between the musculoskeletal human model and the power tool, a simulation model of the workload is created by building a screwdriver model in MATLAB (R2022b) Simulink multibody package based on the cordless screwdriver (Festool cordless impact drill PDC 18/4, Festool GmbH, Wendlingen am Neckar, Germany). The cordless screwdriver is represented with adjustable dimensions and distances for components such as the battery, handle, motor and gearbox, and drill chuck, as illustrated in Figure 3. The masses and dimensions of these components are determined and assigned according to the specifications of the selected screwdriver. The moments of inertia are calculated with MATLAB (R2022b), considering the simplified geometry of the components. Additionally, external process forces and torques are considered based on experimental data obtained during the screw in process. For a detailed description of the model structure and the determination of the interaction forces and torques, refer to the comprehensive description provided by Sanger et al. [38].

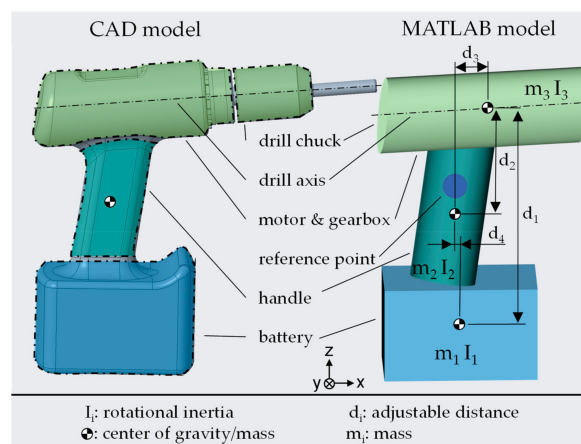


**Figure 3.** Multibody model of the power tool [38]. For the implementation of the co-simulation model a CAD based MATLAB Simscape model of a screwdriver with adjustable distances of the components is used.



### 2.2. Concept of the Co-Simulation Model

Based on the submodels, the realization of the co-simulation model is divided into three consecutive steps as depicted in Figure 4. After a general adjustment of the submodels, their interactions with the user are determined in the co-simulation and the influence on the human body is shown by musculoskeletal analyses. These results form the basis for design options on the technical systems.

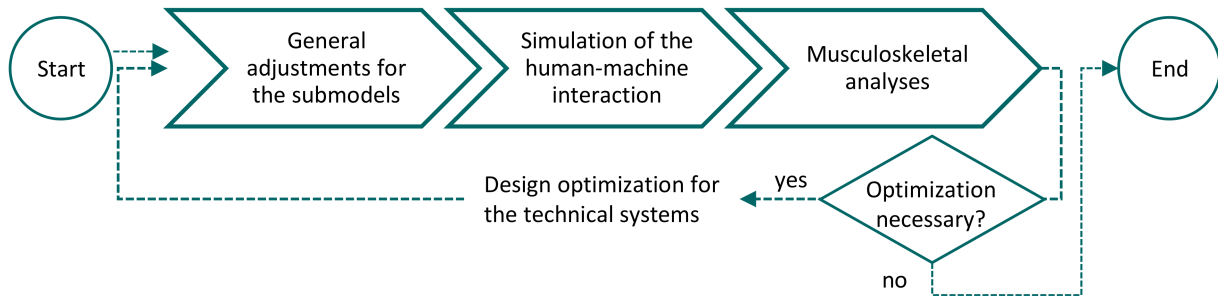


**Figure 4.** Co-simulation process for mapping the human–machine interaction of support systems. The co-simulation process for mapping the human–machine interaction of support systems consists of three consecutive steps, which can be repeated if optimization for the technical systems is required.

#### 2.2.1. General Adjustments for the Submodels

Before simulating and evaluating the human–machine interactions between the user and the technical support systems, some general adjustments to the submodels for the specific use case have to be applied, which are summarized in Figure 5, in order to enable the derivation of design options for different users and variations of the technical systems. The musculoskeletal human model has to be adjusted to the anthropometry of the subject, which includes the segment lengths of body parts and the weight of the subject. The adjustment of the musculoskeletal human models, the so-called scaling, can be done either based on manual measurements of the subject’s individual proportion lengths or more conventionally via an optical motion capture system based on attached markers on the body [39], the so-called marker-based scaling. Either way, the correct representation of the subject in the musculoskeletal human model is needed to derive plausible design optimizations of the technical systems for the user.

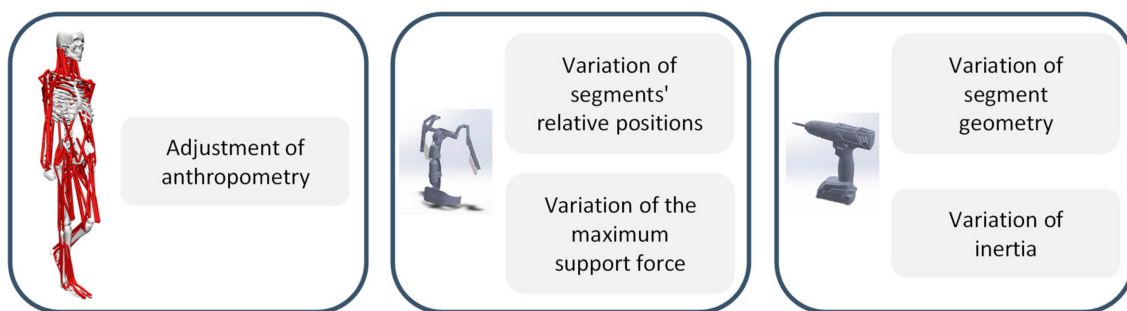


**Figure 5.** Adjustment options for the submodels. By adjusting the submodels, design options of the technical systems can be represented in addition to different potential users and design variations.

The technical systems can be adjusted based on the user and the desired design condition. For the exoskeleton model, its structure and control settings can be varied as described in Section 2.1.2. Furthermore, new options for the structure design and the control strategy can be implemented during an iterative development process and evaluated via the co-simulation model. Besides the exoskeleton, design variations can also be performed on the power tool. Therefore, the geometry of the single components can be adjusted as well as their inertial properties. Consequently, design options, which are to be considered

in the context of the product development of the technical systems, can be implemented at this point.

### 2.2.2. Simulation of the Human–Machine Interaction in the Co-Simulation Model

Based on the general adjustments of the human model and the models of the technical systems, the co-simulation, depicted in Figure 6, can be conducted. Therefore, interfaces between the human model and the technical systems are defined.

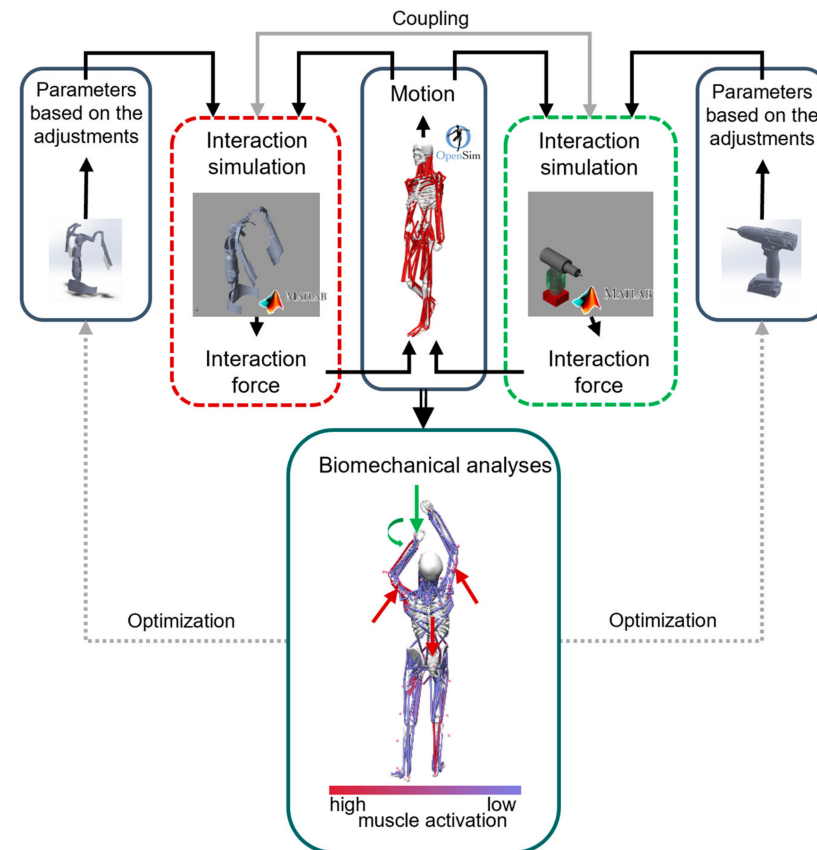


**Figure 6.** Structure of the co-simulation model. Building the co-simulation by modelling the interactions between the technical systems and the human model as the base for biomechanical simulations and analyses.

The human’s motion forms the base for the co-simulation. The motion could be recorded with motion capture methods either based on inertial measurement unit (IMU) [40,41] or optical tracking methods [39,42], which can be transferred to the human model in OpenSim. For the implementation of the co-simulation model, the use case of working at and above head height is chosen.

#### Human–Exoskeleton Interface

For dynamic simulation of human–exoskeleton interactions, an interface is created between the human and the exoskeleton model. The interface defines which motions and forces are exchanged between the two submodels, as well as their coordinate systems. The interaction between the human and the exoskeleton model is performed in four steps in the co-simulation model: First, the human motion data required by the exoskeleton are imported from the human model into the exoskeleton model in the form of marker positions and joint angles of the human. Second, the exoskeleton model simulates the behavior of the exoskeleton in response to human motion and the interaction forces at the physical interfaces between the exoskeleton and the human body. Third, the simulated

interaction forces are exported to the human model. Finally, the biomechanical effects of the interaction forces on the human body are exported to the musculoskeletal human model.

Using the shoulder exoskeleton model mentioned above, three interface points are defined in the human model. These are at the back of the pelvis and at the humerus of each arm, respectively, to the lap belt and armrests as physical interfaces between the exoskeleton and the human body. The marker positions of each humerus are required to simulate the movements of the exoskeleton arms. The resulting interaction forces at the armrests and lap belt are applied to the humerus and pelvis, respectively.

#### Human–Power Tool Interface

The interface between the human and the power tool is defined by a reference point located on the palm of the dominant hand of the user. The power tool model determines the load (forces and torques on the human) at this reference point using experimental data from the study described by Sanger et al. [43] as input for the interaction simulation. The model integrates the motion data recorded by the Vicon motion capture system, the ground reaction forces (GRF), and the battery current of the cordless screwdriver. The user's applied push force is calculated from the GRF, while the screwdriver's battery current is used to estimate the process torque applied to the screwdriver during the screw-in process using the correlation model [43].

The parameters of the power tool can be adjusted to evaluate different tool design options during the co-simulation, as shown in Figure 4. The resultant simulated vectorial interaction forces and torques at the reference point are then fed into the human model as input for the musculoskeletal simulation. A comprehensive model description can be found in Sanger et al. [38].

#### Biomechanical Analyses

In the framework of the musculoskeletal analyses, the influence on the human's motion caused by the working application as well as the influence of support systems can be detected and quantified. The biomechanical analysis not only enables a representation of the relief of the human body caused by the support systems, but also illustrates any additional load on the user. This can be quantified by biomechanical parameters such as muscle activation or joint reaction forces. When considering muscle activation, it is not only possible to look at the muscle activity of all muscles cumulatively, but the evaluation of single muscles and their activations can also be carried out. This allows a differentiated view on which muscles are relieved by the technical systems and which may be more stressed. Next to the muscle activation, the joint reaction forces are part of the biomechanical analyses as well. These forces are almost impossible to measure in physical user tests, but can provide conclusions about the user's load on the joints caused by the application and the technical systems. These evaluation criteria are made available by incorporating a musculoskeletal human model into the co-simulation model and can be used to evaluate the influence of different designs of the technical systems on the human body.

### 2.3. Design of the Subject Study to Evaluate the Co-Simulation Model

#### 2.3.1. Recording the Experimental Data

For the evaluation of the co-simulation model, experimental data were collected in a subject study. Three healthy subjects participated in the study and gave written consent for participating in this study. The study was conducted in accordance with the Declaration of Helsinki, and approved by the Institutional Ethics Committee of the Department of Psychology of Helmut-Schmidt University Hamburg (HSU). By building the models based on physically existing technical systems, these systems can be used for collecting experimental data for the evaluation. Accordingly, the exoskeleton Lucy [1] and a cordless screwdriver (Festool cordless impact drill PDC 18/4, Festool GmbH, Wendlingen, am Neckar, Germany) including a power tool datalogger [44] was used for the subject study. The chosen use case was fixing a predrilled wooden component with a screw to

an overhead plywood board. Here, one hand was used to position the predrilled wooden component (non-dominant hand), while the other hand uses the cordless screwdriver to screw (dominant hand). The use case is shown in Figure 7 and the study is described in detail by Sanger et al. [43].

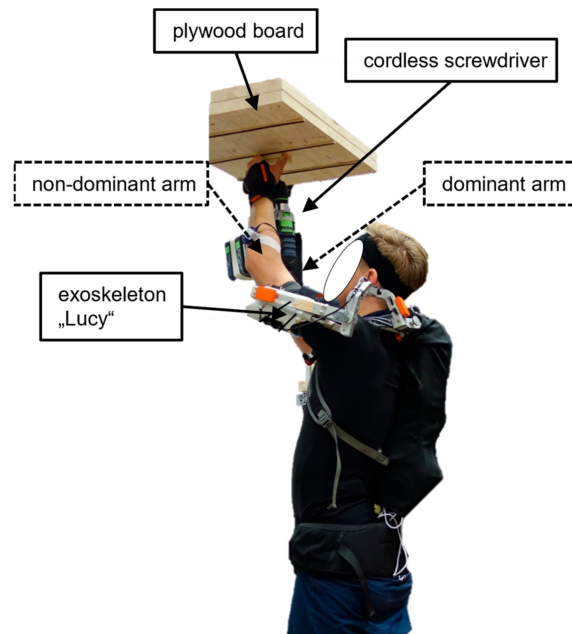


**Figure 7.** Representation of the use case. The use case “Screwing-in above head height with the exoskeleton Lucy and a cordless screwdriver” is used for the evaluation of the co-simulation model.

For the evaluation of the co-simulation model, the data of three subjects (age:  $24 \pm 3.6$  years, weight:  $74.4 \pm 16.1$  kg, height:  $1.84 \pm 0.03$  m, sex: male) were used. The subjects performed the use case with three different levels of exoskeleton support levels: no support, 50% support, and 100% support. For each support level, ten trials were performed. The movement of the subjects was recorded with the optical motion capture system Vicon (Vicon Bonita, Oxford Metrics Ltd., Oxford, UK), sampled at 100 Hz. The subjects wore a suit with attached markers on bony landmarks and required body parts according to the Plug-in-Gait model by Vicon. Although the Plug-in-Gait model is not a specialized marker model to be used for shoulder motions, as it is primarily used for gait analysis, due to its comprehensive marker attachment at the whole body, it was previously also used for analyzing reaching motions [45] or motions during playing tennis [46] and as comparison tool when analyzing shoulder motion [47]. The ground reaction forces of the subjects were measured using a force plate (AMTI, Advanced Mechanical technology Inc., Watertown, NY, USA), sampled at 100 Hz. In addition, surface electromyography (sEMG) was used to record muscle activations of selected muscles in the upper body while performing the activity for the subsequent evaluation of the co-simulation model. Since the exoskeleton, considered in the co-simulation model, is a support system for the shoulder area, the following muscles are used for evaluation: M. biceps brachii, M. deltoideus, M. latissimus and M. flexor carpi ulnaris. For placement of the sEMG electrodes, SENIAM recommendation was used [48]. These data are related to the maximum voluntary contraction (MVC) of the respective muscle of the test subject and can later be used for comparison with the biomechanical results of the co-simulation.

### 2.3.2. Application of the Co-Simulation Model

The musculoskeletal simulation was carried out with OpenSim 4.3. For each subject, a scaled musculoskeletal human model was created based on the tracked markers and weight of the subjects in a static pose via the ScaleTool in OpenSim. With the scaled models,

the motion of fixing a predrilled wooden component with a screw to an overhead plywood board was executed. This was done by means of the inverse kinematics algorithm that minimizes squared distances between measured markers and virtual markers, resulting in joint angles for every defined degree of freedom in the model. The residual reduction algorithm was not applied, because the attached residual actuators to the pelvis of the models ended up in forces and torques below the threshold for good simulation results provided by the OpenSim experts. For each support level, one out of the recorded ten trials was selected as a representative trial following this process: All failed trials, such as fixing errors where the object did not hold on the ceiling, were excluded beforehand. From the remaining trials, the median curve was determined and the trial closest to the median curve was chosen for further analysis. This selected motion trial was transferred via the interface to the exoskeleton and power tool model to simulate the forces applied by the support systems to the human. By the human-exoskeleton interface, the joint angles in the shoulder (shoulder elevation, elevation angle and shoulder rotation) and the position of various markers required for the reproduction of the exoskeleton movement (humerus\_rup, humerus\_rdn, humerus\_rup, humerus\_rdn, Lucy\_Mleft, Lucy\_MC, Lucy\_Mright, T10) over the representative trial were transferred to the exoskeleton submodel (see Section 2.1.2). The returned data of interaction forces and torques were then applied to the respective interaction points at the pelvis and both humeri of the subject musculoskeletal human model. By the human-power tool interface, the orientations and translations of the power tool recorded by optical motion capture were transferred to the power tool model (see Section 2.1.3). The returned data of interaction forces and torques due to the screwing process with the power tool [38] were then applied to the hand of the model.

### 2.3.3. Biomechanical Analysis

In order to analyze the occurring effects for the muscles at screw-in at and above head-height (i.e., power tool forces and torques to the hand) due to the three exoskeleton support levels (i.e., exoskeleton forces and torques to pelvis and both humeri), the static optimization tool (SO) in OpenSim was applied to the human models. These results were at first checked for plausibility, i.e., if the expected changes in the muscles can be seen due to the exoskeleton support. In a second step, the simulated results were compared to the measured muscle data via sEMG. This would show the reproducibility in reality into the simulation and would therefore show that the co-simulation model can be used to derive design options of the technical systems for users. Since four muscles are captured with sEMG (already mentioned earlier in this chapter): *M. biceps brachii*, *M. deltoideus*, *M. latissimus* and *M. flexor carpi ulnaris*, the analyses will focus on these muscles. Furthermore, these muscles are the main ones that are affected in the investigated use case of working at and above head height and these are also even possible to be captured via sEMG. The *M. triceps brachii*, which is also heavily stressed in this use case, cannot be captured via sEMG due to the presence of the armrest at the position the electrodes would be required. However, we did not perform a muscle strength adjustment for each subject, so we did not compare the real muscle activations captured via MVC-sEMG, but rather the curves of the occurring muscle forces in the models with the captured muscle activations. The muscles equipped with sEMG are split in multiple muscles in OpenSim to represent the complete range of action by the real muscle. Thus, in the analysis we merged the results of the muscle parts to one muscle. For this, the weighted sum was applied, meaning that the load on every muscle part was taken into account with a fraction depending on its maximum isometric force compared to the sum of maximum isometric forces of all muscle parts.

## 3. Results

To evaluate the co-simulation model, the courses of the simulated muscle forces of the selected muscles for all three support levels are examined first. The results are compared between the three test subjects and checked for plausibility. Selected simulated muscle



force curves are then compared to the muscle activation curves measured using sEMG. When assessing the results, the focus lies on the dominant side of the respective subject.

### 3.1. Muscle Force Curves Simulated by the Co-Simulation Model

In order to evaluate the results of the co-simulation, the courses of the simulated muscle forces of all three subjects are compared with each other for all three exoskeleton support levels. Figure 8 shows an overview of the results.

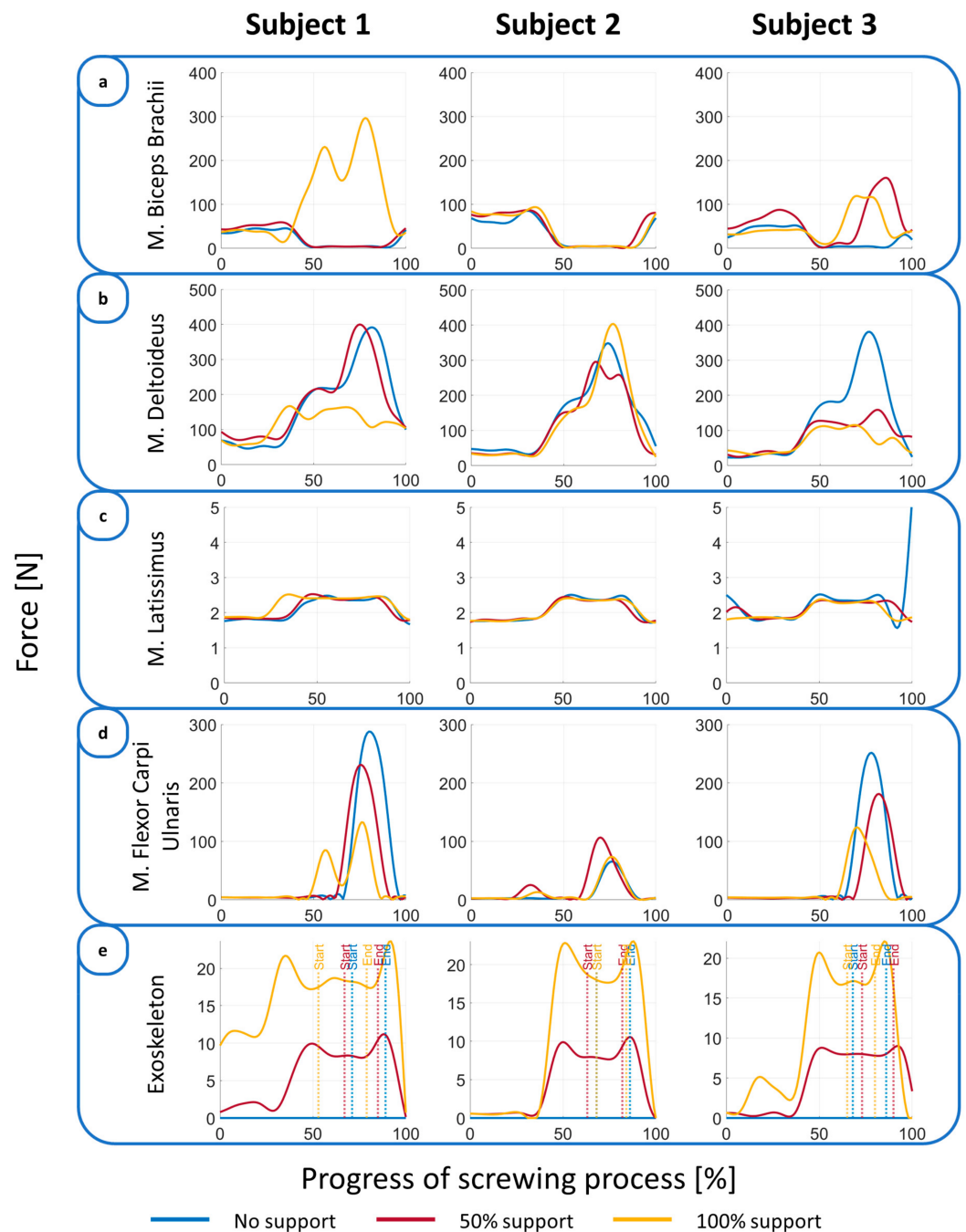


**Figure 8.** Simulated muscle forces. The courses of the muscle forces of the dominant side simulated using the co-simulation model. The graph shows the curves for the selected muscles (a–d) considering all three support levels (no support, 50% and 100% support) and the absolute support forces of the exoskeleton (e). The dashed line indicates the start and end of the screwing process for the respective support level.

For the *M. biceps brachii*, the curves of the three subjects show great similarity, particularly in the range up to approximately 45% of the progress (before the screwing process). The muscle forces remain below 100 N for all three subjects. During the screwing process, subject 1 in particular shows a high muscle force with 100% support. However, the muscle forces of subject 3 also increase in the supported cases compared to the unsupported case.

All three subjects show high muscle forces in the *M. Deltoideus*, particularly during the screwing process. Subject 1 and 3 showed a remarkable reduction in muscle force due to the use of the exoskeleton support.

The *M. latissimus* shows low muscle force in all three subjects, although this increases slightly in all of them during the screwing process. Only slight differences in the simulated muscle force can be seen between the different exoskeleton support levels in all three subjects.

For the *M. flexor carpi ulnaris*, all three subjects show low muscle force before the screwing process. Only subject 2 shows an increase in muscle load after the screwing process in the simulations with support. During the screwing process, the muscle forces are increased in all three subjects, whereby the use of 100% support level usually reduces the muscle force.

### 3.2. Comparison of Simulated Muscle Force Curves with Measured Muscle Activations

The courses of the simulated muscle forces are now compared with the muscle activations measured by sEMG for the selected muscles, as the main focus of the co-simulation model right now is the reproduction of the real occurrences into the virtual model. Figure 9 shows the comparison of the simulation results to captured sEMG activation results for all three subjects. Looking at the *M. biceps brachii*, the curves of the muscle forces roughly match the captured muscle activation. For subject 1, the course of the measured muscle activation also shows a similar activation for all support levels before the screwing process. During the screwing process, the force or activation decreases with no support and 50% support level. The increase in muscle force during the screwing process at the full support level of the exoskeleton is also shown by an increase in the measured muscle activation, but not with that excessive peak. For subject 2, the complete reduction in the screwing phase is not really represented by the measured sEMG data. However, a muscle reduction for the 100% support level can be seen; the 50% support level measured muscle activation stands out in negative way. The unusual rises of forces in *M. biceps brachii* force at 50% and 100% support level for subject 3 are also represented in the captured sEMG data.

The *M. deltoideus* shows overall a pretty good agreement of the simulated muscle forces with the measured muscle activations. For subject 1, the reduce in force of the 100% support level is also existing in the sEMG captured data, but not to such an extent. For subject 3 at no support level, a muscle activation was recorded at the beginning of the movement and not during the screwing process.

A comparison of the muscle force curves of the *M. latissimus* with the measured muscle activation shows good agreement, as the curves of all subjects show. It can also be seen that both the simulated muscle forces and the activation are very low. The small increase during the screwing process is present in both, the simulated muscle forces and the captured muscle activations.

The curves for the *M. flexor carpi ulnaris* show that an increase in force and activation occurs both before and during the screwing process. In the simulation, however, the increase before the screwing phase is lower than during the screwing process. The increases in the measured activations appear to be similar at both times. It can also be seen that the differences between the various support levels are not large, both in the simulation and in the measurements. However, the results between the simulation and the measurement differ slightly. While the support level of 50% causes the lowest activation in the screwing process in the measurement data, the simulation shows the highest muscle forces here.

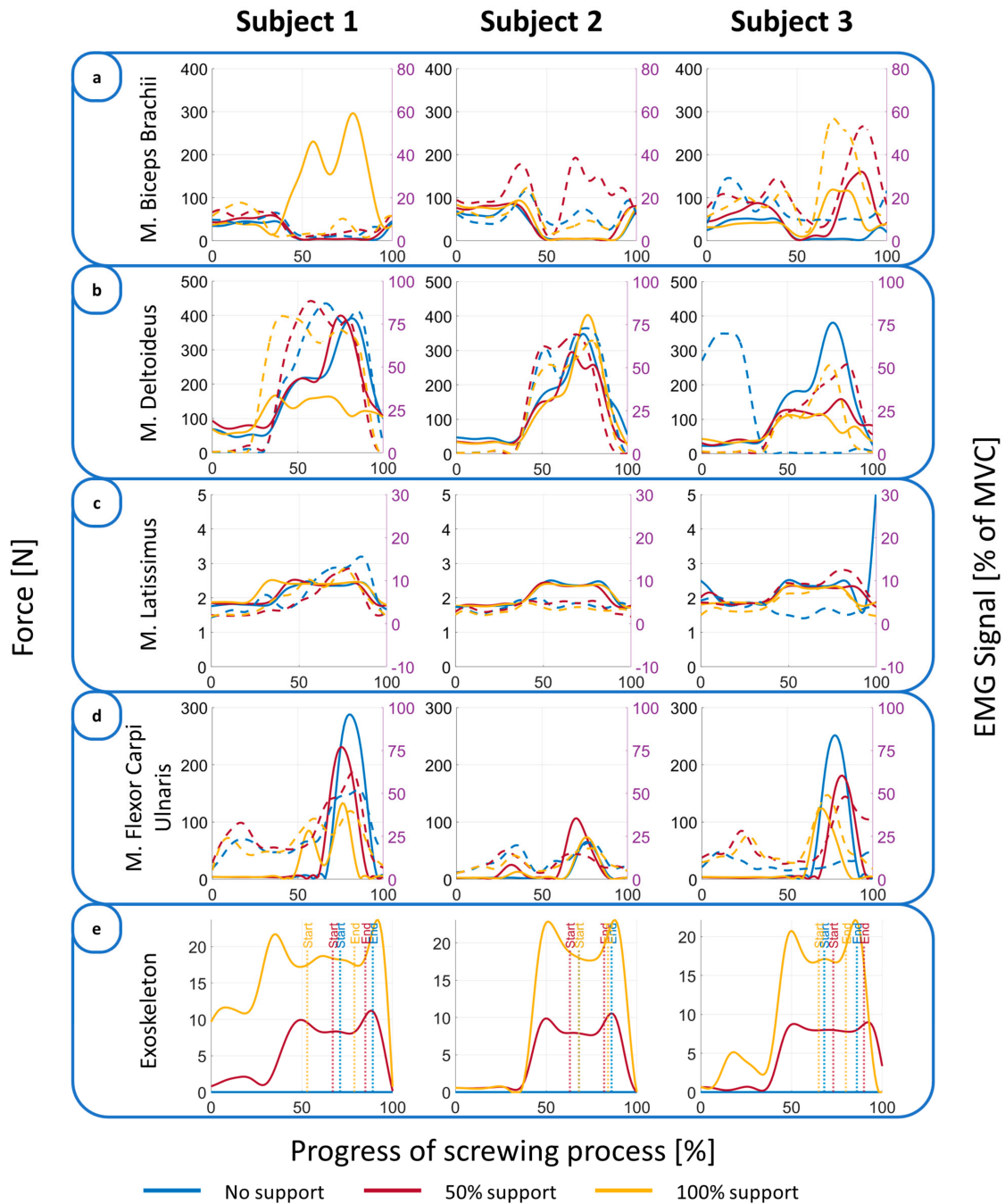


**Figure 9.** Comparison of simulated muscle forces (solid lines) and measured muscle activation via MVC-sEMG (dashed lines) for the three support levels at each subject. Comparison of the courses of the simulated muscle forces with the measured muscle activations of the selected muscles (a–d) for all subjects considering all three support levels (no support, 50% and 100% support) and the absolute support forces of the exoskeleton (e).

#### 4. Discussion

The aim of the provided publication was the setup of a co-simulation model from a musculoskeletal human model and models of technical support systems (in this case an exoskeleton and a power tool) in order to enable the derivation of design options for the technical support systems. The potential of the presented co-simulation model is highlighted when analyzing the simulation results and by comparing the simulation data from the co-simulation model with measurement data collected in a subject study.

A comparison of the simulated muscle forces at all three support levels for all three subjects showed that the results are plausible. For muscles such as the *M. deltoideus* shoulder muscle (see Figure 8), a reduction in the user load due to the exoskeleton support is to be expected, as the exoskeleton used is a shoulder support system [1]. This is also reflected in the simulation. The fact that other muscles, such as the *M. biceps brachii*, sometimes experience increased muscle forces due to the support can also be considered plausible. The use of exoskeletons can sometimes cause higher strain on muscle areas that are not the focus of the relief. Another explanation could also be that the human neuromuscular control strategy alters. With varying boundary conditions, the use of other muscles for the same motion can be the effect. According to the use case of overhead drilling, subjects may rely in the non-supported situation more on one muscle and with increasing exoskeleton support, another muscle can be recruited more. Thus, not only a reduction in load is accomplished by an exoskeleton, but also a re-structuring of muscle recruitment patterns can occur, which has to be aware during design of the exoskeleton. There are, however, some exceptional simulation results differing from other results like the results for the *M. deltoideus* in the supported situations (50% and 100% support level) for subject 2 compared to subject 1 and 3. At this stage, the co-simulation model is mainly able to reproduce the reality into the virtual world. In a next step, the co-simulation model can be used to derive design alternatives for the technical systems from the simulation into the reality.

Thus, the co-simulation model should ideally replicate the curves of muscle loads in the simulation, i.e., the real occurrences in the simulation by the co-simulation model. In many cases, the curves are in good agreement, especially regarding the principal shape of the curves. Special aspects, such as a strong increase in the simulated force of the *M. biceps brachii* with a support level of 100% for subject 1 and for subject 3 at 50% and 100% support level (see Figure 9) are usually also shown in the measured data. Other implications like the poor influence on the *M. latissimus* by the use case itself and further by the assistance of the exoskeleton are also shown in the simulation. The overhead drilling depicts a use case, which does not really cause load for the *M. latissimus*, which is shown by the sEMG. Indeed, it is comparatively easy to capture the *M. latissimus* via sEMG, respecting the use case with exoskeleton, and, thus, an interesting information, whether the co-simulation model simulates any non-existing loads in the musculoskeletal human models. Due to the correct simulated representation of low loads on *M. latissimus*, in the further evaluation more loaded muscles in the back at the investigated use case will be analyzed, like the *M. levator scapula*. However, in some comparisons there are also some deviations noticeable between simulation and measurements. Thus, it can be seen that implicit positive simulation results with actually clear implications that could possibly be derived are not verified by the captured data, as for the *M. biceps brachii* of subject 1 or *M. deltoideus* of subject 3. The reasons for these effects could be assigned to multiple error sources, which could be due to the not really error-safe MVC-EMG measurement method or also due to errors in the co-simulation method or the single elements of the model, which cannot be definitively identified at this stage and has to be investigated in further evaluations. Nevertheless, some key findings like the detectable reduction of the *M. deltoideus* load due to the exoskeleton support, the non-loading of the *M. latissimus* or even the identification of special aspects like the increase of *M. biceps brachii* load, which is verified by the sEMG measurement, show the potential of the co-simulation model that it could be used as a tool to adjust parameters of the technical support systems in the virtual worlds in order to derive recommendations for design alterations of the technical support system regarding the user's needs. A validation of the co-simulation is, indeed, still pending.

Nevertheless, the simulated results mainly replicate the reality for the investigated use case, implying a good representation of the reality by the co-simulation model. With this verification, alterations of the exo support can be done virtually, which can then be evaluated with co-simulation model. When the desired effects occur for the musculoskeletal

human model, the new exo support can be realized to result in an improved comfort for the user. The same can also be done with alterations at the power tool in the virtual, e.g., mass alteration or mass redistribution, resulting in a different mass center and inertia, which can then also be transferred to reality.

Despite the promising results, limitations must also be pointed out. For an initial evaluation of the co-simulation model, a study with three subjects was conducted. A higher number of subjects would further increase the significance of the evaluation with regard to the variance in the anthropometry of the subjects. In addition, some abnormalities in the simulation results might be rather linked to other reasons with an increased number of subjects. Also, only four muscles were respected when analyzing the effects of the exoskeleton and power tool. There are many muscles around the shoulder joint responsible for the complex motion of the shoulder, which are influenced by the load of the power tool and the assistance of the exoskeleton. However, in this first verification step, the effects for the main muscles, which were also even able to be captured due to the presence of the exoskeleton, should have been analyzed and used for the evaluation of the co-simulation model. The other muscles will be analyzed in future investigations, which also includes the analysis of activation of agonist and antagonist muscles. Furthermore, measurement errors can occur when conducting subject studies. As the selected application involves a very dynamic movement, measurement uncertainties can occur due to the movement. Examples of this could be masking of markers during movement recording and slippage or poor skin contact of sEMG electrodes. Lastly, the strength of the musculoskeletal human models of the subjects was not adjusted due to the high effort and time required for modelling and capturing relevant data, but rather the common scaling process of OpenSim was used. Thus, a comparison of muscle activations in total between simulated and captured data was not conducted. For the evaluation of the co-simulation model, the curves of the simulated muscle forces are qualitatively compared with the measured muscle activation, which only allows for an evaluation of basic effects occurring in the co-simulation method. In the future, the muscle forces of the human model could be adapted for specific subjects to improve the validity of the results through a quantitative comparison.

## 5. Conclusions

In conclusion, we presented a co-simulation model integrating a musculoskeletal human model and models of an exoskeleton and power tool. The paper describes the structure of the co-simulation model with the mapping of the interactions between the submodels. The evaluation of the co-simulation model by a subject study completes the paper and emphasizes the potential of the co-simulation model for product development. Due to the virtual depiction of the human-machine interaction, the co-simulation model could be a tool for the digital, user-centered development process of the technical systems. By embedding the technical systems as digital models, they could be varied virtually. The design of the technical systems as well as the maximal support of the exoskeleton can be implemented and the influence of these variations on the human body can be evaluated without physical prototypes or experimental studies with participants. As a result, variations of the technical systems can be tested early in the development process and product design decisions can be made on a better-founded basis. The use of the co-simulation model for the simulation-based assessment of different design options for technical systems like exoskeletons or power tools will be part of future research, where the adjustment of model parameters and the evaluation of resulting effects in a user-friendly way is in focus. Furthermore, the co-simulation model could be extended by a connection between the power tool and the exoskeleton via an information exchange to determine the timing of support from the exoskeleton based on the system state of the power tool, which will also be part of the future research. In addition, taking into account more real-world settings into the co-simulation model, like dynamic interactions between the human model and the submodels, which have impacts on the conducted motion behavior of subjects, is a possible research direction in future and allows for the identification of limits for the



co-simulation model with respect to input parameters and the general robustness, e.g., in the form of a sensitivity analysis.

**Author Contributions:** Conceptualization: C.M., J.S. and Z.Y., methodology (co-simulation model): C.M., J.M., J.S. and Z.Y., software: D.S. and C.L. (human model), J.S. (power tool model), Z.Y. (exoskeleton model), validation: C.M. and D.S., formal analysis: C.M., D.S., C.L. and J.M., investigation: C.M., D.S., C.L., J.S. and Z.Y., resources: C.M., J.S. and Z.Y., data curation: C.M., J.S. and Z.Y., writing—original draft preparation: C.M., D.S. and C.L., writing—review and editing: J.S., Z.Y., A.L., S.M., R.W., S.W. and J.M., visualization: C.M., C.L., J.S. and Z.Y., supervision: J.M., project administration: S.M., R.W. and S.W., funding acquisition: S.M., R.W., S.W. and J.M. All authors have read and agreed to the published version of the manuscript.

**Funding:** This research was funded by the German Research Foundation (DFG). The authors gratefully acknowledge the financial support of project 435242218 (WA 2913/41-1, MA 5940/11-1, and WE 6430/3-1).

**Institutional Review Board Statement:** The study was conducted in accordance with the Declaration of Helsinki and approved by the Institutional Ethics Committee of the Department of Psychology of Helmut-Schmidt University Hamburg (HSU).

**Informed Consent Statement:** Informed consent was obtained from all subjects involved in the study.

**Data Availability Statement:** The data that support the findings of this study are available from the corresponding author upon reasonable request.

**Conflicts of Interest:** The authors declare no conflicts of interest.

## References

- Otten, B.M.; Weidner, R.; Argubi-Wollesen, A. Evaluation of a Novel Active Exoskeleton for Tasks at or Above Head Level. *IEEE Robot. Autom. Lett.* **2018**, *3*, 2408–2415. [\[CrossRef\]](#)
- Alabdulkarim, S.; Nussbaum, M.A. Influences of different exoskeleton designs and tool mass on physical demands and performance in a simulated overhead drilling task. *Appl. Ergon.* **2019**, *74*, 55–66. [\[CrossRef\]](#) [\[PubMed\]](#)
- De Looze, M.P.; Bosch, T.; Krause, F.; Stadler, K.S.; O’Sullivan, L.W. Exoskeletons for industrial application and their potential effects on physical work load. *Ergonomics* **2016**, *59*, 671–681. [\[CrossRef\]](#) [\[PubMed\]](#)
- Rimell, A.N.; Notini, L.; Mansfield, N.J.; Edwards, D.J. Variation between manufacturers’ declared vibration emission values and those measured under simulated workplace conditions for a range of hand-held power tools typically found in the construction industry. *Int. J. Ind. Ergon.* **2008**, *38*, 661–675. [\[CrossRef\]](#)
- Fournier, B.N.; Lemaire, E.D.; Smith, A.J.J.; Doumit, M. Modeling and Simulation of a Lower Extremity Powered Exoskeleton. *IEEE Trans. Neural Syst. Rehabil. Eng. Publ. IEEE Eng. Med. Biol. Soc.* **2018**, *26*, 1596–1603. [\[CrossRef\]](#) [\[PubMed\]](#)
- Franke, N.; Piller, F.T. Key research issues in user interaction with user toolkits in a mass customisation system. *Int. J. Technol. Manag.* **2003**, *26*, 578. [\[CrossRef\]](#)
- Almenara, M.; Cempini, M.; Gómez, C.; Cortese, M.; Martín, C.; Medina, J.; Vitiello, N.; Opisso, E. Usability test of a hand exoskeleton for activities of daily living: An example of user-centered design. *Disabil. Rehabil. Assist. Technol.* **2017**, *12*, 84–96. [\[CrossRef\]](#)
- Björing, G.; Johansson, L.; Hägg, G.M. Choice of handle characteristics for pistol grip power tools. *Int. J. Ind. Ergon.* **1999**, *24*, 647–656. [\[CrossRef\]](#)
- McGibbon, C.A.; Brandon, S.C.; Brookshaw, M.; Sexton, A. Effects of an over-ground exoskeleton on external knee moments during stance phase of gait in healthy adults. *Knee* **2017**, *24*, 977–993. [\[CrossRef\]](#)
- Van Engelhoven, L.; Poon, N.; Kazerooni, H.; Rempel, D.; Barr, A.; Harris-Adamson, C. Experimental Evaluation of a Shoulder-Support Exoskeleton for Overhead Work: Influences of Peak Torque Amplitude, Task, and Tool Mass. *IIEE Trans. Occup. Ergon. Hum. Factors* **2019**, *7*, 250–263. [\[CrossRef\]](#)
- Wartzack, S.; Schröppel, T.; Wolf, A.; Miehling, J. Roadmap to Consider Physiological and Psychological Aspects of User-product Interactions in Virtual Product Engineering. *Proc. Des. Soc. Int. Conf. Eng. Des.* **2019**, *1*, 3989–3998. [\[CrossRef\]](#)
- Alipour, P.; Daneshmandi, H.; Fararuei, M.; Zamanian, Z. Ergonomic Design of Manual Assembly Workstation Using Digital Human Modeling. *Ann. Glob. Health* **2021**, *87*, 55. [\[CrossRef\]](#)
- Grobelny, J.; Michalski, R. Preventing Work-Related Musculoskeletal Disorders in Manufacturing by Digital Human Modeling. *Int. J. Environ. Res. Public Health* **2020**, *17*, 8676. [\[CrossRef\]](#)
- Saraswat, P.; Andersen, M.S.; Macwilliams, B.A. A musculoskeletal foot model for clinical gait analysis. *J. Biomech.* **2010**, *43*, 1645–1652. [\[CrossRef\]](#) [\[PubMed\]](#)
- Kainz, H.; Graham, D.; Edwards, J.; Walsh, H.P.J.; Maine, S.; Boyd, R.N.; Lloyd, D.G.; Modenese, L.; Carty, C.P. Reliability of four models for clinical gait analysis. *Gait Posture* **2017**, *54*, 325–331. [\[CrossRef\]](#) [\[PubMed\]](#)

16. Ikeda, A.; Kurita, Y.; Ogasawara, T. Product usability estimation using musculoskeletal model. In Proceedings of the 2010 3rd IEEE RAS&EMBS International Conference on Biomedical Robotics and Biomechatronics, Tokyo, Japan, 26–29 September 2010; pp. 307–312. [\[CrossRef\]](#)
17. Jeang, A.; Chiang, A.J.; Chiang, P.C.; Chiang, P.S.; Tung, P.Y. Robust parameters determination for ergonomical product design via computer musculoskeletal modeling and multi-objective optimization. *Comput. Ind. Eng.* **2018**, *118*, 180–201. [\[CrossRef\]](#)
18. Rasmussen, J.; Boocock, M.; Paul, G. Advanced musculoskeletal simulation as an ergonomic design method. *Work* **2012**, *41*, 6107–6111. [\[CrossRef\]](#)
19. Peruzzini, M.; Carassai, S.; Pellicciari, M.; Andrisano, A.O. Human-centred design of ergonomic workstations on interactive digital mock-ups. In *Advances on Mechanics, Design Engineering and Manufacturing*; Eynard, B., Nigrelli, V., Oliveri, S.M., Peris-Fajarnes, G., Rizzuti, S., Eds.; Lecture Notes in Mechanical Engineering; Springer International Publishing: Berlin/Heidelberg, Germany, 2017; pp. 1187–1195. [\[CrossRef\]](#)
20. Harbauer, C.M.; Fleischer, M.; Bandmann, C.E.M.; Bengler, K. Optimizing Force Transfer in a Soft Exoskeleton Using Biomechanical Modeling. In Proceedings of the 21st Congress of the International Ergonomics Association (IEA 2021); Lecture Notes in Networks and Systems. Black, N.L., Neumann, W.P., Noy, I., Eds.; Springer International Publishing: Berlin/Heidelberg, Germany, 2022; pp. 274–281. [\[CrossRef\]](#)
21. Miller, R.H.; Russell Esposito, E. Transtibial limb loss does not increase metabolic cost in three-dimensional computer simulations of human walking. *PeerJ* **2021**, *9*, e11960. [\[CrossRef\]](#)
22. Yu, J.; Zhang, S.; Wang, A.; Li, W.; Song, L. Musculoskeletal modeling and humanoid control of robots based on human gait data. *PeerJ. Comput. Sci.* **2021**, *7*, e657. [\[CrossRef\]](#)
23. Uchida, T.K.; Seth, A.; Pouya, S.; Dembia, C.L.; Hicks, J.L.; Delp, S.L. Simulating Ideal Assistive Devices to Reduce the Metabolic Cost of Running. *PLoS ONE* **2016**, *11*, e0163417. [\[CrossRef\]](#)
24. Farris, D.J.; Hicks, J.L.; Delp, S.L.; Sawicki, G.S. Musculoskeletal modelling deconstructs the paradoxical effects of elastic ankle exoskeletons on plantar-flexor mechanics and energetics during hopping. *J. Exp. Biol.* **2014**, *217*, 4018–4028. [\[CrossRef\]](#) [\[PubMed\]](#)
25. Chen, W.; Wu, S.; Zhou, T.; Xiong, C. On the biological mechanics and energetics of the hip joint muscle-tendon system assisted by passive hip exoskeleton. *Bioinspiration Biomim.* **2018**, *14*, 16012. [\[CrossRef\]](#) [\[PubMed\]](#)
26. Sawicki, G.S.; Khan, N.S. A Simple Model to Estimate Plantarflexor Muscle-Tendon Mechanics and Energetics During Walking With Elastic Ankle Exoskeletons. *IEEE Trans. Bio-Med. Eng.* **2016**, *63*, 914–923. [\[CrossRef\]](#) [\[PubMed\]](#)
27. Molz, C.; Yao, Z.; Sanger, J.; Gwosch, T.; Weidner, R.; Matthiesen, S.; Wartzack, S.; Miehling, J. A Musculoskeletal Human Model-Based Approach for Evaluating Support Concepts of Exoskeletons for Selected Use Cases. *Proc. Des. Soc.* **2022**, *2*, 515–524. [\[CrossRef\]](#)
28. Molz, C.; Sanger, J.; Yao, Z.; Germann, R.; Matthiesen, S.; Weidner, R.; Wartzack, S.; Miehling, J. Concept of a co-simulation model integrating a musculoskeletal human model and models of an exoskeleton and a power tool to identify design options for the technical systems. In *Abstract Book; CMBBE: Wales, UK, 2021*; p. 75.
29. Linaker, C.H.; Walker-Bone, K. Shoulder disorders and occupation. *Best Pract. Res. Clin. Rheumatol.* **2015**, *29*, 405–423. [\[CrossRef\]](#) [\[PubMed\]](#)
30. Seth, A.; Hicks, J.L.; Uchida, T.K.; Habib, A.; Dembia, C.L.; Dunne, J.J.; Ong, C.F.; DeMers, M.S.; Rajagopal, A.; Millard, M.; et al. OpenSim: Simulating musculoskeletal dynamics and neuromuscular control to study human and animal movement. *PLoS Comput Biol* **2018**, *14*, e1006223. [\[CrossRef\]](#) [\[PubMed\]](#)
31. Miehling, J. Musculoskeletal modeling of user groups for virtual product and process development. *Comput. Methods Biomech. Biomed. Eng.* **2019**, *22*, 1209–1218. [\[CrossRef\]](#)
32. Dumas, R.; Moissenet, F.; Gasparutto, X.; Cheze, L. Influence of joint models on lower-limb musculo-tendon forces and three-dimensional joint reaction forces during gait. *Proc. Inst. Mech. Engineers. Part H J. Eng. Med.* **2012**, *226*, 146–160. [\[CrossRef\]](#)
33. Seth, A.; Dong, M.; Matias, R.; Delp, S. Muscle Contributions to Upper-Extremity Movement and Work from a Musculoskeletal Model of the Human Shoulder. *Front. Neurobot.* **2019**, *13*, 90. [\[CrossRef\]](#)
34. Fritzsche, L.; Galibarov, P.E.; Gartner, C.; Bornmann, J.; Damsgaard, M.; Wall, R.; Schirrmeister, B.; Gonzalez-Vargas, J.; Pucci, D.; Maurice, P.; et al. Assessing the efficiency of exoskeletons in physical strain reduction by biomechanical simulation with AnyBody Modeling System. *Wearable Technol.* **2021**, *2*, e6. [\[CrossRef\]](#)
35. Troster, M.; Wagner, D.; Muller-Graf, F.; Maufroy, C.; Schneider, U.; Bauernhansl, T. Biomechanical Model-Based Development of an Active Occupational Upper-Limb Exoskeleton to Support Healthcare Workers in the Surgery Waiting Room. *Int. J. Environ. Res. Public Health* **2020**, *17*, 5140. [\[CrossRef\]](#)
36. Zhou, L.; Li, Y.; Bai, S. A human-centered design optimization approach for robotic exoskeletons through biomechanical simulation. *Robot. Auton. Syst.* **2017**, *91*, 337–347. [\[CrossRef\]](#)
37. Yao, Z.; Latifi, S.M.M.; Molz, C.; Scherb, D.; Loffelmann, C.; Sanger, J.; Miehling, J.; Wartzack, S.; Lindenmann, A.; Matthiesen, S.; et al. A Novel Approach to Simulating Realistic Exoskeleton Behavior in Response to Human Motion. *Robotics* **2024**, *13*, 27. [\[CrossRef\]](#)
38. Sanger, J.; Wirth, L.; Yao, Z.; Scherb, D.; Miehling, J.; Wartzack, S.; Weidner, R.; Lindenmann, A.; Matthiesen, S. ApOL-Application Oriented Workload Model for Digital Human Models for the Development of Human-Machine Systems. *Machines* **2023**, *11*, 869. [\[CrossRef\]](#)

39. Lund, M.E.; Andersen, M.S.; de Zee, M.; Rasmussen, J. Scaling of musculoskeletal models from static and dynamic trials. *Int. Biomech.* **2015**, *2*, 1–11. [[CrossRef](#)]
40. Slade, P.; Habib, A.; Hicks, J.L.; Delp, S.L. An Open-Source and Wearable System for Measuring 3D Human Motion in Real-Time. *IEEE Trans. Bio-Med. Eng.* **2022**, *69*, 678–688. [[CrossRef](#)] [[PubMed](#)]
41. Stanev, D.; Filip, K.; Bitzas, D.; Zouras, S.; Giarmatzis, G.; Tsaopoulos, D.; Moustakas, K. Real-Time Musculoskeletal Kinematics and Dynamics Analysis Using Marker- and IMU-Based Solutions in Rehabilitation. *Sensors* **2021**, *21*, 1804. [[CrossRef](#)]
42. Afschrift, M.; de Groote, F.; de Schutter, J.; Jonkers, I. The effect of muscle weakness on the capability gap during gross motor function: A simulation study supporting design criteria for exoskeletons of the lower limb. *Biomed. Eng. Online* **2014**, *13*, 111. [[CrossRef](#)]
43. Sänger, J.; Yao, Z.; Schubert, T.; Wolf, A.; Molz, C.; Miehl, J.; Wartzack, S.; Gwosch, T.; Matthiesen, S.; Weidner, R. Evaluation of Active Shoulder Exoskeleton Support to Deduce Application-Oriented Optimization Potentials for Overhead Work. *Appl. Sci.* **2022**, *12*, 10805. [[CrossRef](#)]
44. Dörr, M.; Ries, M.; Gwosch, T.; Matthiesen, S. Recognizing Product Application based on Integrated Consumer Grade Sensors: A Case Study with Handheld Power Tools. *Procedia CIRP* **2019**, *84*, 798–803. [[CrossRef](#)]
45. Nagaraja, V.H.; Bergmann, J.H.M.; Andersen, M.S.; Thompson, M.S. Comparison of a Scaled Cadaver-Based Musculoskeletal Model with a Clinical Upper Extremity Model. *J. Biomech. Eng.* **2023**, *145*, 041012. [[CrossRef](#)]
46. Ahmadi, A.; Rowlands, D.; James, D.A. Towards a wearable device for skill assessment and skill acquisition of a tennis player during the first serve. *Sports Technol.* **2009**, *2*, 129–136. [[CrossRef](#)]
47. Skublewska-Paszowska, M.; Dekundy, M.; Lukasik, E.; Smolka, J. Analysis of two methods indicating the shoulder joint angles using three dimensional data. *Phys. Act. Rev.* **2018**, *6*, 37–44. [[CrossRef](#)]
48. Hermens, H.J.; Freriks, B.; Disselhorst-Klug, C.; Rau, G. Development of recommendations for SEMG sensors and sensor placement procedures. *J. Electromyogr. Kinesiol.* **2000**, *10*, 361–374. [[CrossRef](#)]

**Disclaimer/Publisher’s Note:** The statements, opinions and data contained in all publications are solely those of the individual author(s) and contributor(s) and not of MDPI and/or the editor(s). MDPI and/or the editor(s) disclaim responsibility for any injury to people or property resulting from any ideas, methods, instructions or products referred to in the content.